

Ground Effect Experiments and Model Validation with Draganflyer X8 Rotorcraft

I. Sharf, M. Nahon, A. Harmat, W. Khan, M. Michini, N. Speal, M. Trentini, T. Tsadok and T. Wang

Abstract—Ground effect on rotary aircraft has been studied for many decades. Although a large body of research results is now available for conventional helicopters, this topic is just beginning to receive attention in the unmanned aerial vehicle community, particularly for small size UAVs. The objective of this paper is to assess the applicability of a widely-used ground effect model, developed in the middle of last century, for predicting the ground effect on a small rotary UAV. The particular vehicle employed in this work, the Draganflyer X8, is actuated by 8 propellers arranged in 4 coaxial pairs in a quadrotor configuration and is currently employed for the development of autonomous landing capabilities for UAVs. The aforementioned ground effect model gives an explicit relationship between the thrust produced by a single propeller while operating in-ground-effect and the thrust out-of-ground effect, as a function of the normalized propeller height above ground. A series of experiments was conducted with the propellers of the vehicle on a test stand, and with the X8 vehicle in flight, from which we obtained the in-ground and out-of-ground thrusts. Juxtaposition of our results against the theoretical model points to a stronger ground effect on the X8 vehicle than predicted by theory. Discussion of the assumptions underlying the theory and the experimental procedures and their implications on the results obtained is also included in the paper.

I. INTRODUCTION

The literature on rotary aircraft has long acknowledged the existence of an increase in the lift of the rotor, when it is in close proximity to the ground [7]. This ‘ground effect’ is due to the interaction of the airflow from the rotor with the ground plane that causes a redirection of the flow so it becomes parallel to the ground, thereby, affecting the lift generation by the rotor. As a result, helicopter pilots routinely have to be aware of and contend with this effect when they land their aircraft. It therefore stands to reason that the controller of an autonomous rotary-wing aircraft will likely perform better if it incorporates knowledge of this ground effect, and possibly explicitly compensates for it, rather than deal with it as a disturbance [10].

A. Background

In this paper, we present the results of investigation into the ground effect on a small unmanned aerial vehicle, the Draganflyer X8 shown in Figure 1(a), manufactured by Draganfly Innovations. This platform, weighs 2.5-3 kg, depending on the payload, and is driven by 8 rotors arranged in four

coaxial pairs, analogously to a quadrotor configuration. Our current work with the X8, conducted in collaboration with DRDC-Suffield, focuses on the development of autonomous landing capabilities for the vehicle in urban environments, for a range of landing conditions and surfaces, including stationary and moving targets. Control of the vehicle, however, when it is in proximity to the ground and to other planar surfaces like walls and ceilings, has proven to be challenging for the vehicle auto-pilot, because of the interaction of the air flow generated by the propellers with the environment. As a precursor to the development of better controllers to cope with these disturbances when landing, the present work focuses on the evaluation of the ground effect on the X8 aircraft, in hover conditions, and validation of the commonly cited ground effect model.

One of the early and most frequently referenced models of the ground effect on rotary-wing aircraft was put forward by Cheeseman and Bennett [3] in 1957 and it predicts the ratio of in-ground-effect (IGE) to out-of-ground effect (OGE) thrust for a single rotor operating at constant power, as a function of the rotor height and propeller radius. A significant body of research has been generated since then, investigating experimentally, analytically and computationally different aspects of ground effect on the aerodynamics of the main rotor in conventional helicopters and related effects on the vehicle [9], [6], [4]. In the Unmanned Aerial Vehicles community, in particular, in the research community working with small-size UAVs, this topic has a much shorter history of inquiry. Yu et al. [14] and Lee et al. [8] investigated vision-based autonomous landing of small rotorcraft on fixed and moving platforms, respectively, while considering ground effect. Of most relevance to this work, however, is the study reported by Powers et al. [11] where results are reported from a set of experiments conducted with a micro-quadrotor (76 g weight) demonstrating both the ground and ceiling effects on the vehicle. Their findings indicate that the ground effect begins to manifest itself at heights significantly higher than predicted by Cheeseman and Bennett’s model.

The principal objective of this paper is to assess the applicability of Cheeseman and Bennett’s model of ground effect in hover for the X8 platform. A complete simulator of the X8 platform based on the dynamics model of the vehicle and including thruster and sensor modelling, is currently being developed to test the state estimation and control algorithms for autonomous landing of the vehicle. It is imperative that this simulator incorporates an accurate model of ground effect on the X8 which is the main motivator

A. Harmat, W. Khan, M. Michini, N. Speal, T. Tsadok and T. Wang are with Department of Mechanical Engineering, McGill, Montreal, Canada

I. Sharf and M. Nahon are Professors in the Department of Mechanical Engineering, McGill, Montreal, Canada inna.sharf@mcgill.ca

M. Trentini is Senior Research Scientist, DRDC-Suffield.



(a)



(b)

Fig. 1. Stock X8 and custom X8

for the present work. Section II reviews Cheeseman and Bennett’s ground effect model which predicts the in-ground-effect thrust generated by a rotor. Section III is dedicated to the description of the experimental procedures employed, the test-rigs used, specially-designed hardware and data collection methods. The results of thruster tests on a static test stand, and in flight are presented and discussed in Section IV. Section V concludes the paper with the implications of our findings and proposed future work.

II. GROUND EFFECT MODELING

It is well known that, when a helicopter rotor is operated near the ground, its apparent thrust is increased due to the effect that the ground plane has on the downward flow of the air flowing out of the rotor. Many authors developing models of helicopters and quadrotors have considered this effect [11], [1], [2] using the relation developed by Cheeseman and Bennett [3] for a single propeller operating in proximity to the ground:

$$\frac{T_{IGE}}{T_{OGE}} = \frac{1}{1 - \frac{R^2}{16z^2}} \quad (1)$$

where T_{IGE} is the thrust generated while operating at a height z above the ground, while T_{OGE} is the corresponding thrust generated by the same rotor operating far from the ground, and R is the propeller radius. To develop this relation, Cheeseman and Bennett applied potential flow theory and the method of images to model the interaction between the propeller slipstream and the ground plane. They assumed that the rotor operating near the ground absorbed the same power as the rotor operating out of ground effect.

Cheeseman and Bennett presented (1) as the simplest possible form to account for ground effect. They also presented more comprehensive forms that would consider forward flight velocity and propeller loading. However, the simplest form appears the one most commonly used in the UAV community. Other authors have also proposed more comprehensive approaches, such as the use of Blade Element Momentum Theory (BEMT) or the Free Vortex

method, coupled with the method of images or the surface singularity method [4] to account for the ground plane. These methods can provide more detailed results, including detailed flowfields, but they lack the simplicity of (1). We choose to further investigate the applicability of (1), partly because of its simplicity, and partly because of its widespread use.

While (1) was developed for a single rotor, it is worthwhile to question its application to a coaxial dual-rotor arrangement. The simple momentum theory used to consider airflow through a propeller does not consider the details of that flow—it simply views the propeller as a disc that instantaneously accelerates the flow passing through it. Since the flow details are not considered, it seems reasonable that the coaxial arrangement could itself be viewed as a virtual disc that similarly accelerates the flow. Based on this logic, it would seem that the coaxial propeller arrangement is not a barrier to the use of (1), as long as the underlying assumptions (e.g., constant power) are satisfied.

III. EXPERIMENTAL METHODS AND PROCEDURES

As already noted, the principal objective of the experiments presented in this paper is to evaluate the ground effect model in (1) for predicting the response of the X8 vehicle near the ground. This requires carrying out experiments with the aircraft flying in ground effect, for which we can determine the in-ground-effect and out-of-ground-effect thrusts, T_{IGE} and T_{OGE} for the same power, as per assumptions of (1), as well as the corresponding height of the rotors above the ground (z). In performing the experiments that will be detailed in later sections, the absorbed power could not be measured in flight. The only direct measurement of the propeller operation available was its rotation speed. As well, we were able to deduce the thrust generated by the propellers in a steady hover.

Since it was not possible to ensure the constant power condition in our experiments, an alternative approach is adopted in this work: it imposes a constant rotor speed condition for determining the OGE thrust corresponding

to a particular IGE thrust. Since constant rotational speed is not equivalent to constant power, we investigated the implications of a constant power assumption on the speed relation using momentum theory. We found that, under constant power conditions, the rotational speeds in and out of ground effect would differ by less than 0.5% for all $z > R$. Since the normal landing gear of the X8 ensures that $z > R$, we concluded that constant speed conditions would be nearly identical to constant power conditions, thus allowing the use of (1).

Accordingly, the procedure used to determine the three variables involved in (1) is comprised of the following main elements:

- (i) The thrust generated by the X8 in ground effect flight tests, i.e., T_{IGE} , is determined from the equation of motion for the vehicle in the vertical direction under the assumption of level flight, that is, from the weight of the vehicle and its vertical acceleration (i.e., $T_{IGE} = m(g + \ddot{z})$), or simply from its static equilibrium analogue if a particular constant value of height is maintained. As will be further detailed in Section III-B, one rotor of the X8 vehicle was instrumented with optical sensors to measure the rotation speeds of one rotor pair during the flight tests.
- (ii) An independent series of tests, referred to as thruster identification tests, was carried out with the coaxial rotor pair from the X8 mounted on a specially-designed instrumented static test stand. From these experiments, we obtained a relationship for the thrust generated by the coaxial pair as a function of the rotation speeds of the top and bottom rotors. Using this identified relation with the measured rotation speeds from the ground effect flights with the X8 as per (i), the value of OGE thrust was computed—hence, the constant speed assumption inherent in this method.
- (iii) The rotor height, in particular, the height of the lower propellers, was determined by using a Vicon motion capture system, as described in Section III-B.

A. Thruster Identification Experiments

1) *Identification Test Setup Overview:* In order to identify the characteristics of the X8 rotors, which are a counter-rotating coaxial propeller pair, a versatile test stand was constructed. The test stand is intended to mimic the X8 top and bottom propellers mounted to the arm of the vehicle so that experiments involving varying rotor speeds can be performed in a controlled and well-instrumented environment, and the thrust and torque generated by the rotor can be measured. The experimental setup facilitates the study of a variety of interesting operating situations including single-propeller thrust/torque testing, two-propeller operation (with associated flow-field coupling between them), and even proximity effects for the rotor. Because the experiments conducted with the test stand are intended for the identification of the thrust vs. rotation speed relationship for the rotors of X8, the motors selected to drive the propellers and dimensions of the test rig closely match those of an X8 arm.

The test stand, shown in Figure 2 is comprised of two identical brushless direct-current (BLDC) motors mounted on slightly different axes to reproduce the small inclination of the motor axes on the X8. The X8 top and bottom rotors (see Table 1) are fitted onto the motors such that the rotors spin in opposite directions in normal operation. The spacing between the top and bottom rotor discs on X8 is maintained exactly on the test stand. The motors are individually controlled with electronic speed controllers (ESCs), which are powered by a lithium-polymer battery. The motor/rotor assemblies are fastened to a metal arm dimensioned similarly to the folding arms of X8, which extends down to a force/torque measurement unit. The entire assembly is placed on a moveable frame so that it can be easily positioned in relation to obstacles, although this was not done in the experiments reported here.

2) *Instrumentation:* The test stand incorporates two types of sensors for measuring the performance of the rotors: a force/torque sensor to measure the thrust and torque of the rotor and two optical sensors to measure the rotational speed of the propellers. The same rotor speed sensors are also used on the X8 vehicle to measure the top and bottom propellers' speeds during the ground effect flight tests, as described in Section III.B.

Thrust and torque measurement is achieved by an ATI Gamma 6-axis force/torque sensor. The moment arm of the test setup was selected such that the maximum sensing range of the force/torque transducer was exploited. In this way, thrust was measured to ± 0.004 N, corresponding to about 0.06 % of the nominal thrust of the X8 rotor pair. The test arm is connected to the force transducer through rubber grommets to attenuate high frequency vibrations inherent in propeller operation. An averaging filter is sufficient to remove the low levels of remaining high-frequency noise.

The rotor speed sensors were custom designed to meet the requirements of our experiments. It was required that rotor speed measurement be available on the X8 in flight without adding significant weight to the aircraft. The rotor speed had to be measured with high resolution in order to draw meaningful conclusions about changes in thrust due to ground effect, since these changes were not expected to be large in magnitude. The propeller speed sensor designed used a phototransistor to detect the passing of a white and black stripe on the motor casing. Based on documented microcontroller latencies and quartz crystal frequency tolerances, the system can measure rotation time accurate to approximately 5 microseconds, corresponding to an uncertainty of 0.35 RPM at a rotation speed of 2000 RPM.

3) *Thruster Testing Procedure:* Rotational speed data is sent to the control computer from the rotational speed sensors, and the data is timestamped and recorded. At the same time, data from the force/torque sensor is captured and timestamped. The tests are performed with steady state motor speed values, so that data recording latency and slight timestamp mismatch is not a concern. In all, 17 tests were conducted by setting the bottom rotor speed and changing the top rotor speed from 1500 RPM to 3900 RPM in increments

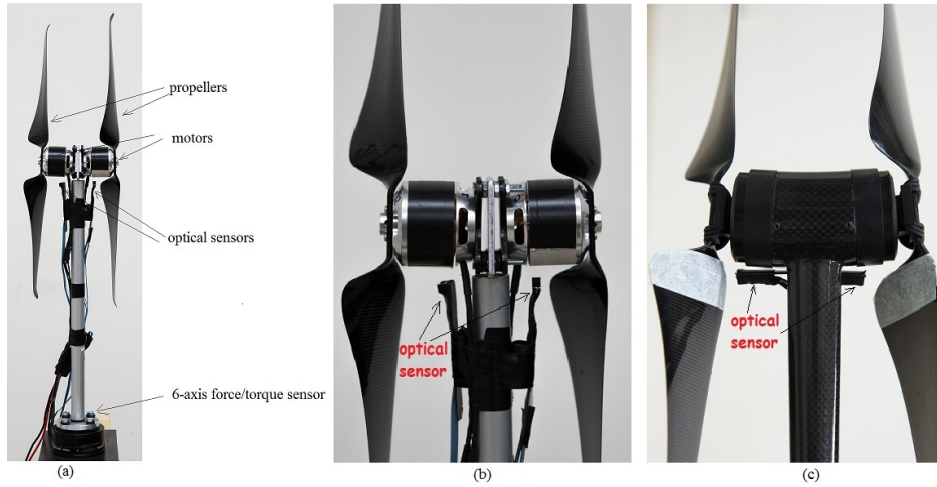


Fig. 2. (a) thruster identification test stand; (b) optical sensor mounted on the test stand; (c) optical sensor mounted on X8

of 150 RPM. This was repeated for the same bottom rotor speed settings. Combinations where the difference between top and bottom rotor speeds was greater than 1500 RPM were excluded, producing a total of 247 test data sets. After all the tests, data is post-processed and amalgamated to yield a relationship between thrust and rotational speed for the particular test configuration. The results of post-processing are discussed in Section IV.A.

B. Ground Effect Experiments

A number of modifications were made to the off-the-shelf X8 vehicle, first with the goal of developing autonomous landing capabilities for it and secondly, specifically for the purpose of conducting the ground effect experiments. The latter are discussed in this section in detail, following a brief description of the vehicle’s configuration and relevant parameters. The procedure used for the flight tests is given at the end of this subsection.

1) *X8 Platform Overview*: Figure 1(a) shows a picture of the X8 platform as it was originally procured from Draganfly Innovations, without the payload camera. The vehicle consists of a central platform with four folding arms that snap into place for assembly. A motor pod containing two motors is located at the end of each arm, which spins counter-rotating propellers (top and bottom) of different diameters for a total of eight rotors (four rotor pairs). The vehicle is equipped with lightweight carbon fibre skid-type landing gear, and is powered by a lithium polymer battery. Table I lists the important parameters of the vehicle.

The X8 comes equipped with several sensors to enable varying degrees of autonomy: an inertial measurement unit (IMU), a 3-axis magnetometer, a barometric pressure sensor, and a GPS receiver. The aircraft’s autopilot allows the operator to select the desired level of autonomy: manual throttle, altitude hold, or position hold. In manual throttle mode, the aircraft uses the IMU and magnetometer to maintain level flight and a selected heading, and the operator controls all other flight inputs including height via throttle. In altitude

TABLE I
X8 AIRCRAFT PARAMETERS

Vehicle mass	2.025 kg	
Arm length	0.331 m	
Top rotor diameter	0.404 m	
Bottom rotor diameter	0.380 m	
Rotor vertical spacing	0.100 m	
Top rotor clearance (tip to tip)	0.064 m	
Bottom rotor clearance (tip to tip)	0.085 m	
Top rotor nominal RPM	2347	
Bottom rotor nominal RPM	2577	
Bottom rotor height above ground	Stock configuration	0.200m
	Lowered configuration	0.073m
Battery capacity	5400 mAh	

hold mode, the aircraft uses the pressure sensor to maintain an altitude setpoint, while the position hold mode can be used to maintain a given 3D position using a combination of the pressure sensor and the GPS receiver.

All of the flight inputs, including autopilot mode selection, are performed using the X8’s included handheld controller, with the exception of the manual throttle mode, which has been disabled on the stock handheld controller. This mode, however, is still present in the aircraft’s onboard autopilot, and was used to fly the X8 in the ground effect experiments by accessing it with third party software that communicates with the aircraft directly.

2) *Modifications for Ground Effect Experiments*: As noted in Section II, the simple model of ground effect, (1) predicts it to be negligible for rotor heights above approximately one propeller diameter [5], while it becomes progressively more significant as the rotor height is reduced. Indeed, when the rotor is at the height equal to one propeller radius, the ground effect results in a 6.7% increase in thrust relative to the same power thrust out-of-ground effect [13]. The off-the-shelf configuration of X8, as well as the customized configuration for the autonomous landing research place the bottom propellers of the vehicle at 0.20 m above ground, i.e., approximately one rotor radius. Therefore, in order to generate sufficient data to validate the ground effect

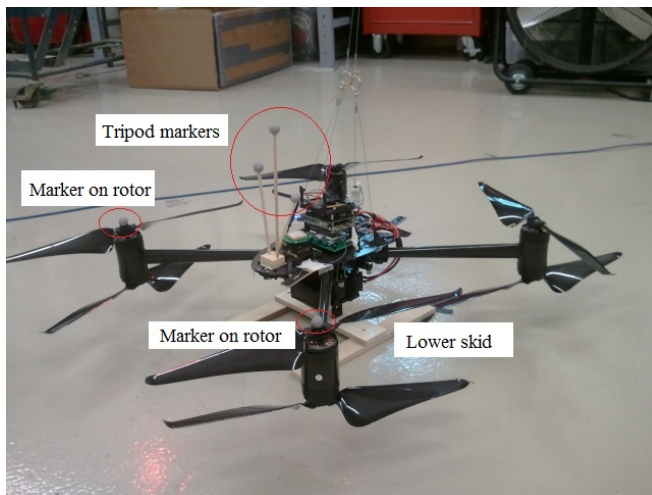


Fig. 3. X8 with lower skid and markers

model and given that flying the vehicle close to the floor bears a high risk of collision and vehicle damage, the original landing gear of X8 was replaced with a shorter wooden skid construction (see Figure 3). This resulted in the bottom propeller height of 0.073 m when the vehicle is on the floor, thus allowing us to fly the vehicle close enough to the ground to collect sufficient data in ground effect.

To produce accurate measurements of the height z values required for validation of (1), a motion capture system from Vicon was employed. The Vicon setup includes six cameras mounted to the ceiling in the Aerospace Mechatronics Laboratory¹ in a circumferential arrangement. The X8 platform was equipped with a set of retro-reflective markers indicated in Figure 3: a tripod of markers was mounted on the vehicles body and two additional markers were affixed to the centers of top rotors. With this setup, the Vicon system generates very accurate position and orientation measurements of the defined body-fixed frame of the vehicle from which the bottom rotor height values can be computed. In the ground effect experiments reported in this paper, the vehicle was kept very close to level in flight and the rotor height value was assumed to be the same for all four bottom propellers, calculated directly from the Vicon z -position values with appropriate offset.

The last modification made to the vehicle for the purpose of ground effect experiments is the mounting of the optical sensor on one of the four rotor pairs. The optical sensor used for this purpose is the same as the one used for the thruster identification experiments, as described in Section III.A. The sensors were mounted to one of the motor pods with adhesive tape to measure the speeds of top and bottom propellers of one rotor pair.

3) *Flight Tests*: A series of ground-effect experiments was performed with the X8. Initial tests were conducted by flying the aircraft using the altitude hold mode of the

¹All experiments reported in this manuscript were conducted in AML (Aerospace Mechatronics Laboratory) in the Department of Mechanical Engineering at McGill University.

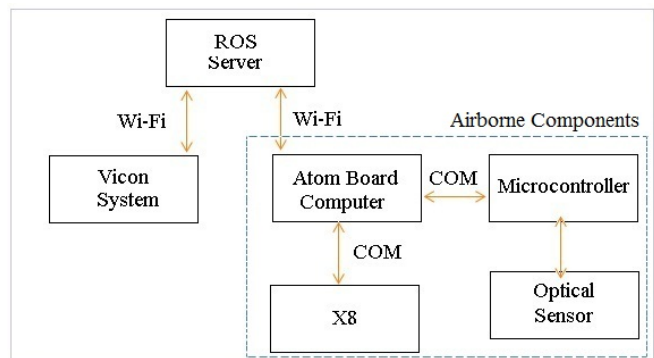


Fig. 4. Data acquisition and communication in ground effect tests

remote controller supplied with the vehicle, but these resulted in a very poor altitude regulation when the vehicle descended into ground effect. This was found to be due to erratic data from the pressure sensor that provides height feedback to the controller—presumably as a result of the strong pressure fluctuations in the propeller slipstream when the vehicle approaches the ground. As a result, later flights were carried out by flying the aircraft in the manual throttle mode, resulting in a significant improvement in the vehicle’s altitude regulation when flying close to the ground. Results from four flight tests are reported in this paper, all obtained using the manual throttle mode and executed approximately as follows. After take-off, the aircraft was flown to an altitude of approximately 1.5 m where it was stabilized in hover for approximately a minute. This was followed by a descent in several intervals into the ground effect, with a pause at each interval, until the final landing.

A schematic showing data acquisition and streaming during the ground effect tests is included in Figure 4. A desktop computer running ROS (Robot Operating System) [12] collects the data from X8 and Vicon System through Wi-Fi. The Atom processor board from Ascending Technologies has been added to the X8 platform for the purpose of implementing autonomous control and SLAM algorithms on the platform. In the ground effect experiments, the Atom board is used to collect the IMU and pressure sensor data from the autopilot of X8 through a serial port, as well as the rotation speed of the propellers from the microcontroller acquiring optical sensor measurements, also through a serial port. Note that in the ground effect experiments, the aircraft is operated primarily in steady-state, hovering at different heights and with slow transitions between the heights. Thus, although rotation speed information is collected from one rotor pair only, we assume the same contribution to the out-of-ground thrust of the vehicle for the other three rotors. All measured data transmitted to the ROS server are timestamped and the server synchronizes itself, the Atom board computer and the Vicon system controller.

IV. EXPERIMENTAL RESULTS

A. Thruster Identification

As noted earlier, the first set of experiments was conducted on a single coaxial pair of motor/propellers from the vehicle on a test stand, to provide data for thrust out-of-ground effect, for a variety of propeller speeds. The test stand allowed simultaneous measurements of propeller speeds and thrust/torque generated by the coaxial pair. The propeller speeds were generally not at torque-balanced conditions, reflecting the fact that the coaxial pairs of the X8 are not always operated in this condition.

Initial experiments focused on characterizing the top and bottom propellers individually. Many prior works have shown that the thrust of a single propeller can be written as $T = C_T \rho R^4 \omega^2 = b \omega^2$, where the thrust coefficient C_T and rotor radius R are constants for a given rotor. Tests were conducted on the top and bottom propellers in isolation, confirming this relation and yielding values for b_{b_0} and b_{t_0} shown in Table II. Using $\rho = 1.225 \text{ kg/m}^3$, $R_b = 0.190 \text{ m}$ and $R_t = 0.202 \text{ m}$, then results in $C_{Tb} = 0.0345$ and $C_{Tt} = 0.0257$ for our rotors. If these two propellers were operated independently, they would be expected to generate a total thrust of

$$T = 5.5 \times 10^{-5} \omega_b^2 + 5.2 \times 10^{-5} \omega_t^2 \quad (2)$$

where ω_b and ω_t are the rotation speeds of bottom and top rotors, respectively.

When two propellers are placed in a coaxial arrangement, the outflow of one is directed to the inflow of the second. In this arrangement, it is also well known that the thrust of both propellers will be affected, and that the total thrust will be significantly less than would be obtained if the two propellers were operated separately. This is mainly due to the reduced thrust of the downstream propeller operating in the propwash of the upstream propeller.

Tests were performed to measure the total thrust produced by a coaxial thruster pair at various top and bottom propeller speeds. The resulting database of measurements was post-processed with the goal of identifying the thrust vs. rotor speeds relationship for the X8 coaxial pair. To maintain consistency with the quadratic form obtained for the single-propeller tests, the data was used to find best-fit coefficients in the equation

$$T = b_b \omega_b^2 + b_t \omega_t^2 \quad (3)$$

with the resulting coefficients shown in Table II. Based on these coefficients, we find that, for a situation in which the top and bottom propellers spin at the same speed, the thrust would be reduced by 14% relative to the independent configuration, clearly demonstrating the loss of thrust of the coaxial arrangement. At the same time, comparison of the coefficients obtained with propellers operated separately to the respective values for a coaxial arrangement indicates, at first glance, that in the coaxial case, the upstream (top) propeller is adversely affected by the downstream one (bottom), while the downstream propeller is unaffected by the upstream propeller. With the help of a blade element momentum model, this counterintuitive result was eventually traced to

TABLE II
IDENTIFIED THRUST PARAMETERS OF X8

	Single propeller model parameters	Coaxial rotor parameters
Curve fitted values [Ns ² /rad ²]	$b_{b_0} = 5.5 \times 10^{-5}$ $b_{t_0} = 5.2 \times 10^{-5}$	$b_b = 5.5 \times 10^{-5}$ $b_t = 3.7 \times 10^{-5}$
RMSE (root mean square error)	bottom: 0.0798 top: 0.0593	0.0625

the fact that the bottom propeller loses thrust in proportion to the square of the speed of the upper propeller. This reinterpretation of the data demonstrates that, as expected, the downstream propeller is the one that suffers loss of thrust in the coaxial arrangement.

Table II also shows the quality of the fit obtained by this equation in terms of rms error. Other forms of equations were fit to the data, with no significantly better fit relative to (3). The experimental data and the fitted model are shown in Figure 5 which demonstrates that the model provides a very good match with the measurements. This model is therefore used in the next section to compute the out-of-ground thrust for the ground effect experiments.

B. Ground Effect Results

1) *Angular Speeds of Coaxial Propellers:* We begin by presenting the angular speeds of the top and bottom propellers, as a function of height, collected during one of the four tests. The raw optical sensor measurements, being quite noisy, were processed with a nonlinear regression to obtain the two curves in Figure 6. The horizontal axis used in this and later plots shows the height normalized by the rotor radius (of the bottom propeller). Because the tests are carried out in quasistatic conditions, the rotor thrust produced by a single rotor pair can be taken to be one quarter of the X8 weight, at every point in Figure 6. This then demonstrates that the propellers need to spin considerably faster when the aircraft is far from the ground, than when it approaches the ground, in order to generate the same thrust. A key reason for presenting the results in this form is to draw a comparison with the analogous results obtained for a micro-quadrotor [11]. Similarly to those findings, the rotor speed profiles indicate that the influence of the ground is apparent at heights corresponding to $z/R = 5$ —significantly higher than what is predicted by the model in (1).

2) *IGE Thrust Normalized by OGE Thrust:* We now consider the ratio of the IGE to OGE thrusts obtained for the ground effect experiments. We recall that the IGE thrust is computed from the vehicle weight with the addition of the vertical acceleration term obtained from the IMU data, although the latter was found to be negligible for our tests. The out-of-ground-effect thrust is calculated with the measured in-flight rotor speeds, using the fitted model in Section IV.A and the ratio of the two thrusts is computed. Figure 7 shows the four curves corresponding to the four tests, obtained again with nonlinear regression analysis of the raw results.

Two important observations can be made based on Figure

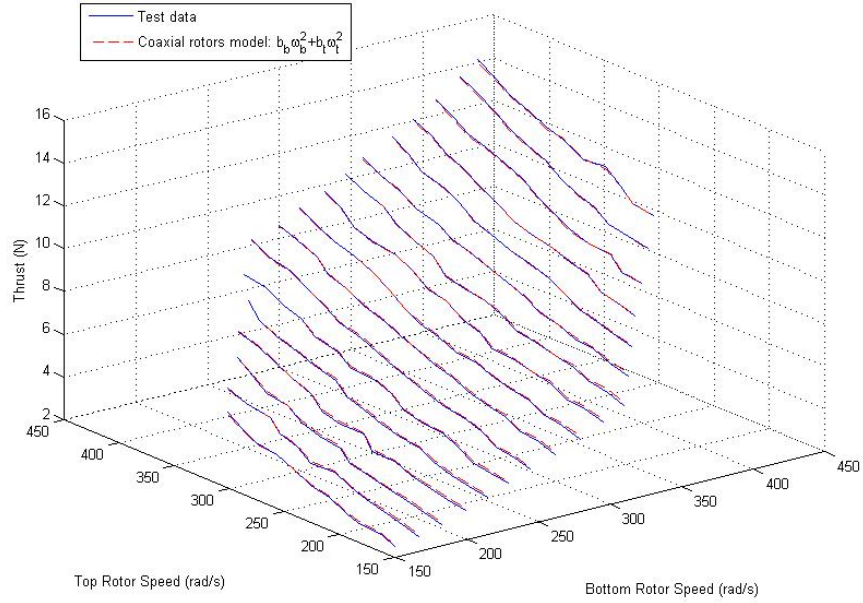


Fig. 5. Test data and fitted thrust model

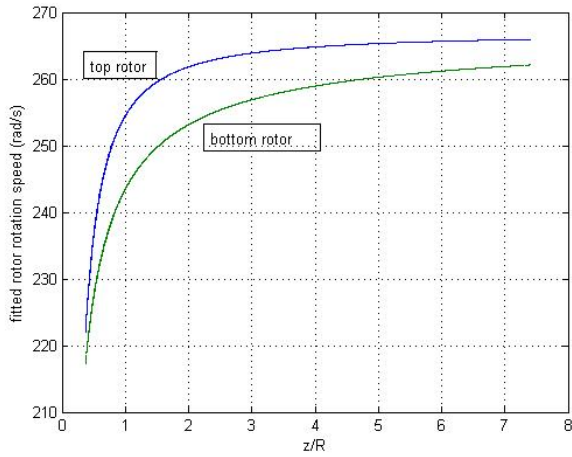


Fig. 6. Rotor speeds vs. normalized height

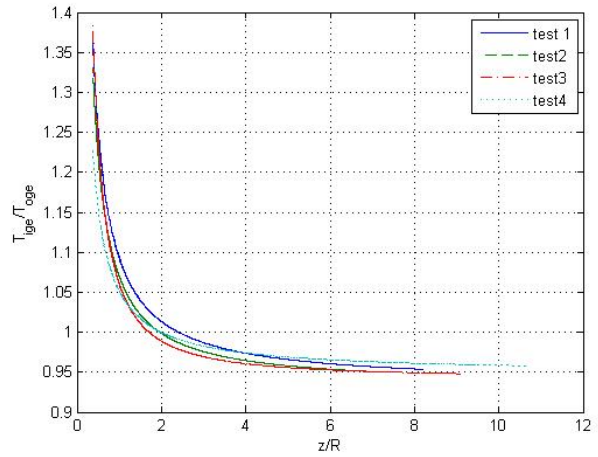


Fig. 7. Test Ground Effect vs. Empirical Ground Effect

7: (i) there is good agreement between the results obtained from the four tests; (ii) all four curves exhibit a consistent off-set between the actual out-of-ground thrust and the expected OGE thrust computed based on the measured rotor speeds and the identified model of a coaxial rotor. In principle, we should expect these curves to converge to unity at large values of z/R . This offset, or discrepancy from unity, ranges from 3.4% to 4.6% for the four tests, averaging at 3.9%. Approximately 2% of this discrepancy was accounted for by the decrease in thrust resulting from the air flow impinging on the skid landing gear jutting into the rotor slipstream (this was verified by a separate experiment where the landing gear was removed completely).

The remaining discrepancy can likely be attributed to

the interference between rotor pairs when operating in a quadrotor arrangement. While basic momentum theory predicts that there should be no interaction, as long as the propeller footprints do not overlap, more detailed analysis [4] has shown that, the flows of non-overlapping rotors can interact when they are less than 1.5 diameters apart (center to center), leading to changes in total thrust. The rotors of X8 are mounted at 1.16 diameters apart, making the interaction very likely.

3) *IGE Thrust Normalized by Actual OGE Thrust*: To correct for the above-noted discrepancy, the data of each test in Figure 7 was normalized by the OGE thrust measured in that same test. This then ensured that all the curves would converge to unity at large values of z/R . The resulting curves

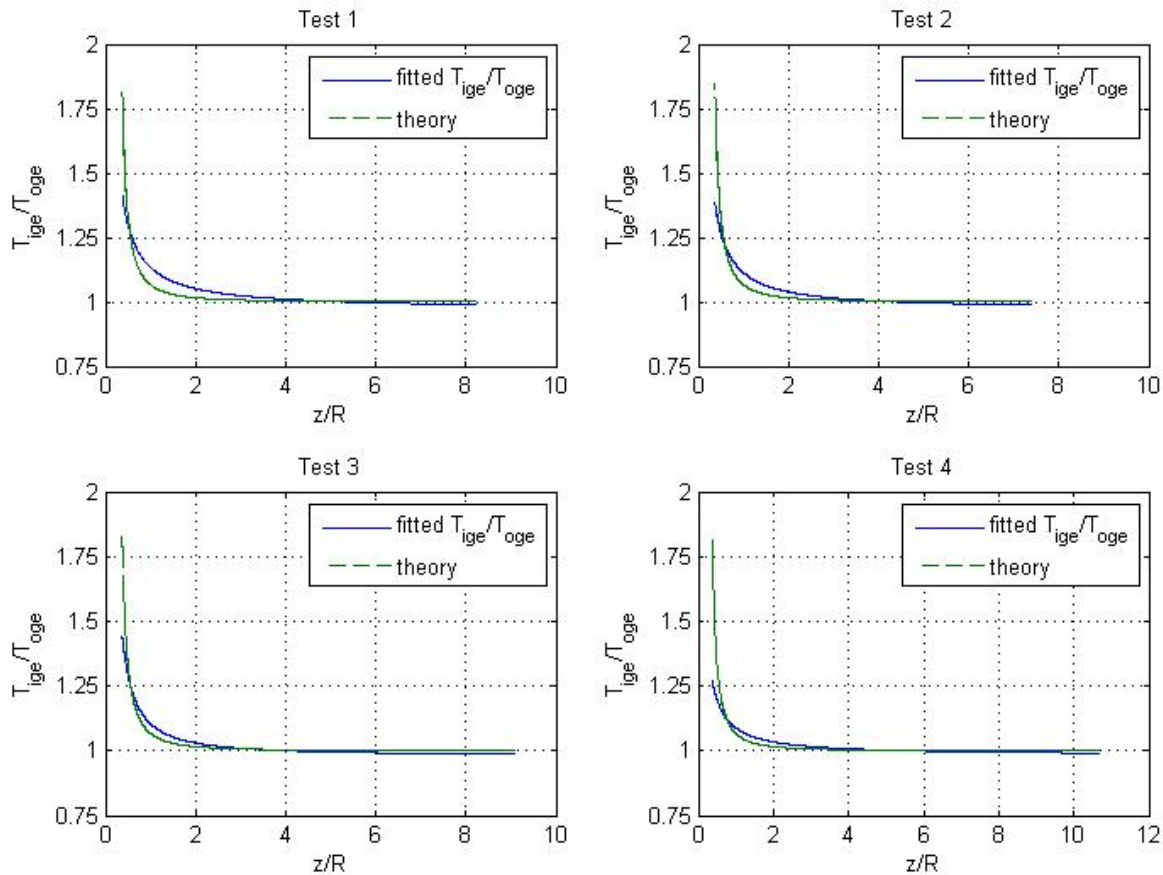


Fig. 8. Empirical GE vs. Calibrated Test GE

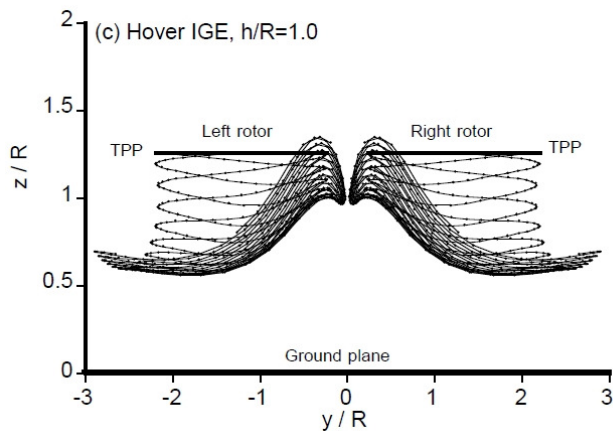


Fig. 9. Flowfield of Tandem Rotors in Ground Effect[4]

are shown in Figure 8 and compared to the model prediction of (1). Qualitatively, the agreement between Eq. (1) and our experimental results is good, but there are some distinct differences.

Our results show a consistently higher increase in thrust in the range $0.5 < z/R < 3$. This range is important, as

it represents the heights when the vehicle is about to land (the off-the-shelf landing gear normally comes into ground contact at $z/R \approx 1$). This indicates that the ground effect is apparent at higher altitudes in our data than in (1). To explain these results, we focused on two aspects: the fact that Cheeseman and Bennett's model relates to a single isolated propeller, while our experiments used multiple coaxial pairs, in a quadrotor arrangement. As alluded earlier, the coaxial arrangement was not deemed to be relevant, since a coaxial pair can be viewed as a single virtual propeller of appropriate induced velocity. It was concluded that the quadrotor arrangement was the most likely explanation for the increased ground effect. A more detailed explanation for this can be found in the work of Griffiths and Leishman[4]. When the four rotor pairs are placed in a quadrotor arrangement, *and* in ground effect, this can lead to strong flow interactions [4] of the slipstream flow between the rotors. Whereas a single propeller would have an axisymmetric flowfield in which the flow splays out radially in all directions when it encounters the ground plane, Figure 9 shows the interaction of the flow fields of two tandem rotors near a ground plane. In this dramatically different flowfield between the two rotors at the ground plane, sometimes called a fountain effect, the flow between the rotors reverses back up through the rotors.

This reversal should lead to a stronger ground effect for this arrangement than for the single rotor, but Griffiths and Leishman[4] do not provide any data to quantify this.

V. CONCLUSION

The research reported in this paper focused on the experimental evaluation of a commonly-used relation for ground effect of rotors in proximity to the ground, using an 8-rotor UAV. It was found that our results gave good qualitative correspondence to the equation, but that the measured ground effect appears stronger at a given distance from the ground. The analytical equation predicts that ground effect only becomes apparent when the aircraft rotor is at the height of two rotor radii from the ground while our results show that the effect is noticeable at three rotor radii in the thrust plots and at five rotor radii in the propeller speed plots. We believe that the cause of this lies in the complex flowfield interactions that exist due to the quadrotor arrangement of the thrusters. The strong ground effect is expected to make control of landings more difficult than in a conventional single-rotor helicopter due to the larger changes of behavior between in- and out-of-ground-effect. Future work will aim at confirming our conjecture by running additional tests for a single rotor pair in proximity to the ground, which we expect will yield results closer to those predicted by theory.

ACKNOWLEDGMENTS

The research described in this manuscript was funded through contract W7702-11-5122 from DRDC-Suffield. We gratefully acknowledge the assistance of PhD candidate Mikael Persson for setting up the Vicon system for the ground effect flight tests.

REFERENCES

- [1] S Bouabdallah and R Siegwart. *Advances in Unmanned Aerial Vehicles*, chapter Design and Control of a Miniature Quadrotor, pages 171–210. Springer Press, 2007.
- [2] A. R. S. Bramwell, George Taylor Sutton Done, and David Balmford. *Bramwell's Helicopter Dynamics*. AIAA, 2001.
- [3] I. C. Cheeseman and W. E. Bennett. The effect of the ground on a helicopter rotor in forward flight. Technical report, Aeronautical Research Council, 1957.
- [4] Daniel A. Griffiths and J. Gordon Leishman. A study of dual-rotor interference and ground effect using a free-vortex wake model. In *Proc. of the 58th Annual Forum of the American Helicopter Society*, Montreal, Canada, 2002.
- [5] Wayne Johnson. *Helicopter Theory*. Dover Publications Inc., New York, 1980.
- [6] Ning Kang and Mao Sun. Simulated flowfields in near-ground operation of single- and twin-rotor configurations. *Journal of Aircraft*, 37(2):214–220, 2000.
- [7] Montgomery Knight and Ralph A. Hegner. Analysis of ground effect on the lifting airscrew. Technical Report NACA-TN-835, National Advisory committee for Aeronautics, 1941.
- [8] D. Lee, T. Ryan, and H. J. Kim. Autonomous landing of a vtol uav on a moving platform using image-based visual servoing. In *Proceedings of the IEEE International Conference on Robotics and Automation*, pages 971–976, 2012.
- [9] Joon W. Lim, Kenneth W. McAlister, and Wayne Johnson. Hover performance correlation for full-scale and model-scale coaxial rotors. *Journal of the American Helicopter Society*, 54(3):1–14, 2009.
- [10] Kenichiro Nonaka and Hirokazu Sugizaki. Integral sliding mode altitude control for a small model helicopter with ground effect compensation. In *Proceedings of 2011 American Control Conference*, pages 202–207, San Francisco, CA, USA, June 2011.
- [11] Caitlin Powers, Daniel Mellinger, Alex Kushleyev, Bruce Kothmann, and Vijay Kumar. Influence of aerodynamics and proximity effects in quadrotor flight. In *Proceedings of the International Symposium on Experimental Robotics*, June 2012.
- [12] Morgan Quigley, Ken Conley, Brian P. Gerkey, Josh Faust, Tully Foote, Jeremy Leibs, Rob Wheeler, and Andrew Y. Ng. Ros: an open-source robot operating system. In *ICRA Workshop on Open Source Software*, 2009.
- [13] John Wakinson. *The Art of the Helicopter*. Elsevier Butterworth-Heinemann, Burlington, MA, 2004.
- [14] Z. Yu, K. Nonami, J. Shin, and D. Celestino. 3d vision based landing control of a small autonomous helicopter. *International Journal of Advanced Robotic Systems*, 4(1):51–56, 2007.